

# Bis(azobenzene)-Based Photoswitchable, Prochiral, C<sup>α</sup>-Tetrasubstituted α-Amino Acids for Nanomaterials Applications

Paola Fatás,<sup>[a]</sup> Edoardo Longo,<sup>[b]</sup> Federico Rastrelli,<sup>[b]</sup> Marco Crisma,<sup>[c]</sup>  
Claudio Toniolo,<sup>[b]</sup> Ana I. Jiménez,<sup>[a]</sup> Carlos Cativiela,<sup>[a]</sup> and Alessandro Moretto\*<sup>[b]</sup>

Great interest is currently devoted to molecular or supra-molecular entities that have access to two or more forms, the interconversion of which can be triggered by an external stimulus.<sup>[1]</sup> Several switching systems have been reported that are based on photochromic behavior, resulting in optical control of chirality, fluorescence, intersystem crossing, electrochemically and photochemically induced changes in liquid crystals, thin films, and membranes.<sup>[2]</sup> The design of molecular compounds that exhibit photoinduced magnetization and magnetic transitions is one of the main challenges in the field of materials science because of their potential application to optical memory and switching devices.<sup>[3]</sup> Hence, the construction of new types of optically switchable magnetic compounds that exhibit both large magnetization changes and ferromagnetic order even at room temperature is nowadays an issue of great interest.<sup>[3a,c,4]</sup> Particularly intriguing are photoactive molecules formed on the surface of gold, silver, and platinum nanoparticles. Owing to the high surface-to-volume ratio, the concentration of photoactive compounds compared to the number of metal atoms allows for standard characterization techniques, such as UV/Vis or FTIR absorption spectroscopy, to be employed to detect photochromic switching.<sup>[3b]</sup> Azobenzene ranks among the first photochromic switches used and is still the subject of extensive investigation.<sup>[5]</sup> Its *cis*- and *trans*-isomers (hereafter termed *c* and *t*, respectively) have a different spatial arrangement of the aromatic moieties, and consequently show significantly diverse physical and chemical properties, including dipole moments.

We are currently expanding this field by developing a novel family of C<sup>α</sup>-tetrasubstituted α-amino acids, characterized by two azobenzene moieties covalently linked to the α-carbon atom through a methylene group, to be exploited as photoresponsive building blocks in different systems. These compounds can be viewed as the result of introducing a phenylazo group at either the *para* or *meta* position of the two aromatic side chains in dibenzylglycine (Dbg). These symmetrically substituted, bis(azobenzene)-containing amino acids, bis[*p*-(phenylazo)benzyl]glycine (*pazo*Dbg) and bis[*m*-(phenylazo)benzyl]glycine (*mazo*Dbg), were prepared as the ethyl esters, H-*pazo*Dbg-OEt (**1**), and H-*mazo*Dbg-OEt (**2**), as illustrated for the former compound in Figure 1 I (for synthetic details, see the Supporting Information).

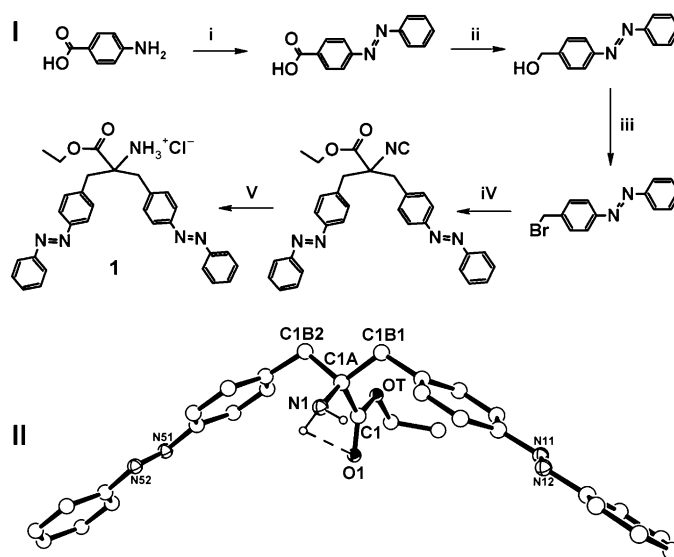


Figure 1. (I) Synthesis of **1**. Reagents and conditions: (i) AcOH, nitrosobenzene, RT, 24 h, 80 %; (ii) THF, LiAlH<sub>4</sub>, RT, 24 h, 93 %; (iii) triphenylphosphine, *N*-bromosuccinimide, THF, RT, 12 h, 91 %; (iv) ethyl isocynoacetate, tetrabutylammonium bisulfate, K<sub>2</sub>CO<sub>3</sub>, 50 °C, 24 h, 96 %; (v) HCl, EtOH, RT, 2 h, 100 %. (II) X-ray diffraction structure of the “albatross-like” compound **1**. The intramolecular (amino) N–H···O = C (ester) H-bond is indicated by a dashed line.

[a] P. Fatás, Dr. A. I. Jiménez, Prof. C. Cativiela  
Department of Organic Chemistry, ISQCH  
University of Zaragoza-CSIC  
50009 Zaragoza (Spain)

[b] E. Longo, Dr. F. Rastrelli, Prof. C. Toniolo, Dr. A. Moretto  
Department of Chemistry  
University of Padova  
via Marzolo 1, 35131 Padova (Italy)  
Fax: (+39)049-827-5829  
E-mail: alessandro.moretto.1@unipd.it

[c] Dr. M. Crisma  
Institute of Biomolecular Chemistry, Padova Unit, CNR  
via Marzolo 1, 35131 Padova (Italy)

Supporting information for this article is available on the WWW under <http://dx.doi.org/10.1002/chem.201102609>.

by condensation of *p*- or *m*-aminobenzoic acid with nitrosobenzene in acetic acid and further elaboration of the carboxylic acid group. The slow evaporation of a CH<sub>2</sub>Cl<sub>2</sub>/MeOH solution of **1** furnished single crystals suitable for X-ray diffraction analysis (Figure 1 II). The backbone of the  $\alpha$ -amino ester adopts an extended conformation [N1-C1A-C1-OT ( $\psi_T$ ) torsion angle:  $-179.8(3)^\circ$ ], which allows for the presence of an intramolecular H-bond ( $C_5$  form) between the N1-H1B nitrogen and the O1 carbonyl oxygen. The occurrence of the fully-extended conformation has been crystallographically documented for other C $^{\alpha\alpha}$ -symmetrically disubstituted glycines, including Dbg, in simple derivatives and peptides.<sup>[6]</sup> The  $\chi^1$  torsion angles about the C1A-C1B1 (*pro-S* side chain) and C1A-C1B2 (*pro-R* side chain) bonds are in the *g*+ [ $62.9(3)^\circ$ ] and the *g*<sup>-</sup> [ $-62.7(3)^\circ$ ] dispositions, respectively. The two azobenzene moieties are in the *t* conformation and are essentially flat, the angle between normals to the aromatic rings in each azobenzene group being  $10.3^\circ$  and  $2.6^\circ$  for the *pro-S* and the *pro-R* chain, respectively. Interestingly, the distance between the terminal carbon atoms of the two side chains is as long as 20.29 Å and the overall shape of the molecule is reminiscent of an albatross.

The isomerization properties induced by light on these bis(azobenzene)-containing amino acids were investigated. First, **1** and **2** were transformed into the free acids bearing an *S*-(trityl)-3-mercaptopropionyl group at the amino function, Trt-S-(CH<sub>2</sub>)<sub>2</sub>-CO-*pazo*Dbg-OH (**3**) (Figure 2 I) and Trt-S-(CH<sub>2</sub>)<sub>2</sub>-CO-*mazo*Dbg-OH (**4**), respectively (Trt = trityl;

for synthetic details, see the Supporting Information). This derivatization was performed to subsequently exploit these compounds as capping layers for metal nanoparticles. The photoswitching capability of **3** and **4** was characterized by UV/Vis spectroscopy, NMR, and reverse-phase HPLC. Both compounds underwent multiple, reversible isomerizations (compound **3**, Figure 2; compound **4**, see the Supporting Information) in a variety of solvents upon irradiation with Vis light (450 nm, *c*→*t*) or UV light (350 nm, *t*→*c*).

Specifically, 0.1 mM solutions of **3** and **4** in MeOH (as well as in several different solvents; data not shown) were irradiated separately at two different wavelengths, 350 and 450 nm, for multiple cycles. Under UV irradiation at 350 nm, the intensity of the strong absorption maximum at 330 nm, typical for the *t* form of the azobenzene moieties, rapidly decreased in both samples while the weak absorption band at 435 nm concomitantly increased (Figure 2 II). The opposite phenomenon occurred when the solutions were subsequently illuminated with Vis light at 450 nm. However, when **3** and **4** were dispersed in a paraffin medium, the *c*↔*t* photoswitch process was blocked. No significant difference was observed between the *para*- and *meta*-substituted compounds. Interestingly, when the photoisomerization process of **3** and **4** was monitored by HPLC up to three isomeric species were detected, as shown in Figure 2 III (inset) for **3**. The peak eluting between the *c* and *t* isomers was attributed to an intermediate state in the *t*→*c* and *c*→*t* interconversion pathways, in which only one of the

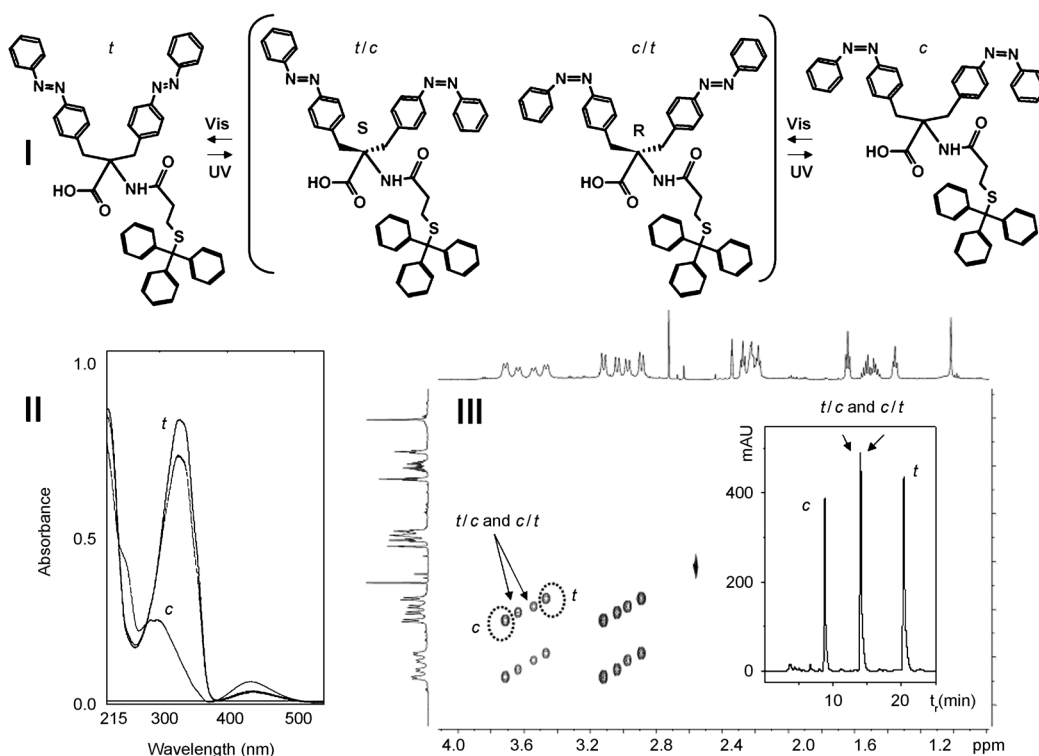


Figure 2. (I) Mechanism of light-driven isomerization for **3** (same mechanism, not shown for **4**). (II) UV/Vis absorption spectra of the multiple, reversible *c*↔*t* isomerization of **3** in a 0.1 mM solution in MeOH. (III) DQF COSY sub-spectrum of **3** in CDCl<sub>3</sub> run after 2 min irradiation at 350 nm (ratio of compounds as in the HPLC profile; III inset), shows the concomitant presence of three isomeric species.

two azobenzene moieties has isomerized. As a consequence of this limited photoswitch, the C<sup>α</sup>-atom becomes chiral and therefore a mixture of two enantiomers (Figure 2I) is generated. The central peak in the chromatogram should then correspond to a racemic mixture of the enantiomeric species formed by isomerization of a single azobenzene unit, namely the *t/c* and *c/t* forms. To confirm our hypothesis of “mono” isomerization, double-quantum filtered (DQF) COSY NMR experiments were carried out on **3** for the all-*t* form, its all-*c* isomer, and a ≈ 1:1:1 mixture of the all-*t*, *t/c* + *c/t* (racemate), and all-*c* isomers generated by 2 min irradiation with UV light. In the latter case, the NMR spectrum (Figure 2III) provides clear evidence for the occurrence of three independent species in a photostationary equilibrium (the geminal -C<sup>β</sup>H<sub>2</sub>- protons in the amino acid side chains become diastereotopic).<sup>[7]</sup> Similar results were obtained for **4** (see the Supporting Information).

This phenomenon was further, albeit indirectly, demonstrated by investigating the photoisomerization of the chiral dipeptide containing the *pazoDbg* residue coupled with L-leucine methyl ester, H-*pazoDbg*-L-Leu-OMe (**5**). In this case, owing to the presence of L-Leu, the intermediate species generated upon isomerization of a single azobenzene unit are diastereomers, H-(*R*)-*pazoDbg*-L-Leu-OMe and H-(*S*)-*pazoDbg*-L-Leu-OMe (Figure 3), and should therefore be distinguishable in the HPLC and NMR experiments. A solution of compound **5** in MeOH in the all-*t* conformation was prepared and the isomerization process under irradiation with UV light was followed by HPLC (Figure 3 II).

tion with UV light was followed by HPLC (Figure 3 II). Beside the two peaks corresponding to the all-*t* and all-*c* forms, two additional peaks of similar intensity were detected and assigned to the diastereomeric dipeptides exhibiting each azobenzene group of the *pazoDbg* residue in a different isomeric state, that is, the *t/c* and *c/t* species in Figure 3I. This “mono” isomerization step was also analyzed by DQF COSY experiments on a ≈ 1:1:1 mixture of all four isomers (Figure 3II). This study demonstrated that the remote L-Leu stereocenter affects all of the diastereotopic -C<sup>β</sup>H<sub>2</sub>- protons, which resulted in a further splitting of the DQF COSY cross-peak patterns as compared to those in Figure 2III. Indeed, these experiments provide evidence for the presence of four independent species in a photostationary equilibrium.

The behavior of different metal nanoparticles conjugated with **3** was next investigated. Au, Ag and Pt nanoparticles (Figure 4I) were prepared by chemical reduction (with NaBH<sub>4</sub>) of HAuCl<sub>4</sub>, AgNO<sub>3</sub>, and H<sub>2</sub>PtCl<sub>6</sub>, respectively, in a CHCl<sub>3</sub>/methanol/water mixture in the presence of **3**.<sup>[8]</sup> According to our TEM analysis (Figure 4II) spherical Ag, Au, and Pt nanoparticles (1.5–4 nm diameter) were obtained. Formation of the **3**-conjugated nanoparticles was confirmed by the UV/Vis absorption spectra, in which weak (due to the small nanoparticle size and the large absorption coefficient of the azobenzene moieties) metal-dependent plasmonic bands were observed.

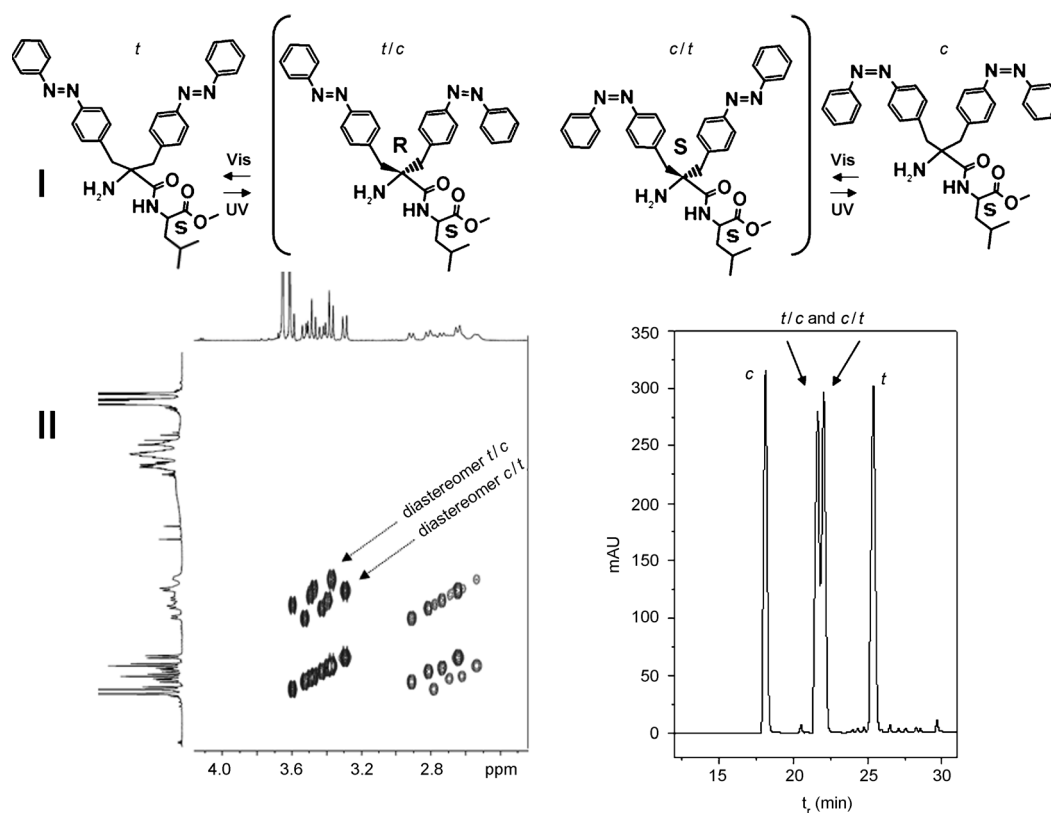


Figure 3. (I) Mechanism of light-driven isomerization for **5**. (II) Left: DQF COSY sub-spectrum of **5** in CDCl<sub>3</sub> run after 3 min irradiation at 350 nm high-lights the concomitant presence of four isomeric species. Right: HPLC profile.

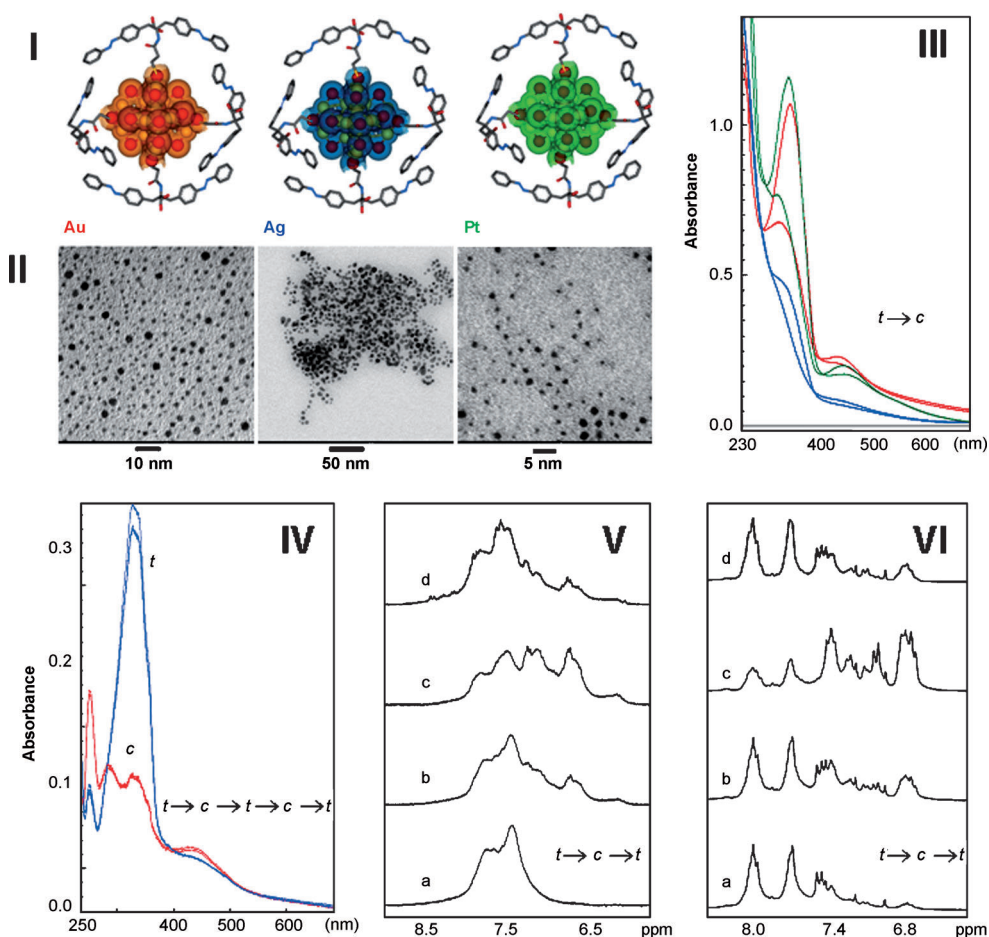


Figure 4. Light-driven isomerization of the **3**-conjugated metal nanoparticles. (I) Representations of AuNp-**3** (left), AgNp-**3** (center) and PtNp-**3** (right). (II) Representative TEM micrographs. (III) UV/Vis absorption spectra of the  $c \leftrightarrow t$  isomerization of Ag, Au, Pt nanoparticles capped with **3** in MeOH. Colors of the curves match those of the corresponding nanoparticle-conjugates in part (I). (IV) UV/Vis absorption spectra for the  $c \leftrightarrow t$  isomerization of AuNp-**3** in a paraffin medium (solid state). (V)  $^1\text{H}$  NMR spectra of AuNp-**3** run after different times of irradiation: (a) 0 min, all- $t$ ; (b) 6 min irradiation at 350 nm; (c) 10 min irradiation at 350 nm, all- $c$ ; and (d) 20 min irradiation at 450 nm. (VI)  $^1\text{H}$  NMR spectra of PtNp-**3** run after different times of irradiation: (a) 0 min, all- $t$ ; (b) 6 min irradiation at 350 nm; (c) 10 min irradiation at 350 nm, all- $c$ ; and (d) 20 min irradiation at 450 nm.

The photoswitch behavior of the conjugates was initially investigated by UV/Vis spectroscopy in solution (Figure 4 III), which allowed us to follow the reversible isomerization process. Then, the Au nanoparticles (AuNp-**3**) were examined in the solid state (dispersed in a paraffin medium; Figure 4 IV), where the photoinduced molecular switch was clearly seen over several cycles of irradiation. For the AuNp-**3** and Pt nanoparticles (PtNp-**3**) the  $c \leftrightarrow t$  isomerization was also studied by NMR (Figure 4 V and VI) and HPLC. In the NMR experiments, part of the complex envelope of broad signals, corresponding to the aromatic protons of both metallic nanoparticles, showed a significant upfield shift during the irradiation process at 350 nm. The irradiation was stopped after 10 min, when the NMR spectra did not change anymore. Then, the NMR tube was irradiated with Vis light for 20 min. At this point, the new NMR signals were almost superimposable to those in the initial spectra recorded before UV irradiation. Monitoring the isomerization process by HPLC (see Supporting Information), it was found that the peak corresponding to the all- $t$  form of

AuNp-**3** (and PtNp-**3** as well) changed its retention time under UV irradiation.

As recently reported by Einaga and co-workers,<sup>[3a,c]</sup> azobenzene-passivated gold nanoparticles show a “controlled” ferromagnetism.<sup>[9]</sup> They demonstrated that this property can be selectively modulated by alternating photoillumination with UV and Vis light (that is, by exploiting  $c \leftrightarrow t$  isomerization) in the solid state. Based on this result, we investigated the magnetic susceptibility  $\chi$  of AuNp-**3** by solution-state NMR at room temperature.<sup>[10]</sup> The method is based on the fact that the resonance frequency for a given nucleus depends, among other factors, upon the volume susceptibility of the medium. We used *tert*-butanol as the inert indicator compound and  $\text{CD}_3\text{OH}$  as the solvent, and focused our attention on AuNp-**3**. This conjugate was subjected to sequential irradiation at 350 nm (5 time points), 450 nm (3 time points) and again 350 nm (3 time points).

The resulting chemical shifts for the *tert*-butanol  $\text{CH}_3$  protons (inner and outer NMR tubes) are reported in Figure 5. The modulation of  $\chi$  as a consequence of irradiation is pro-

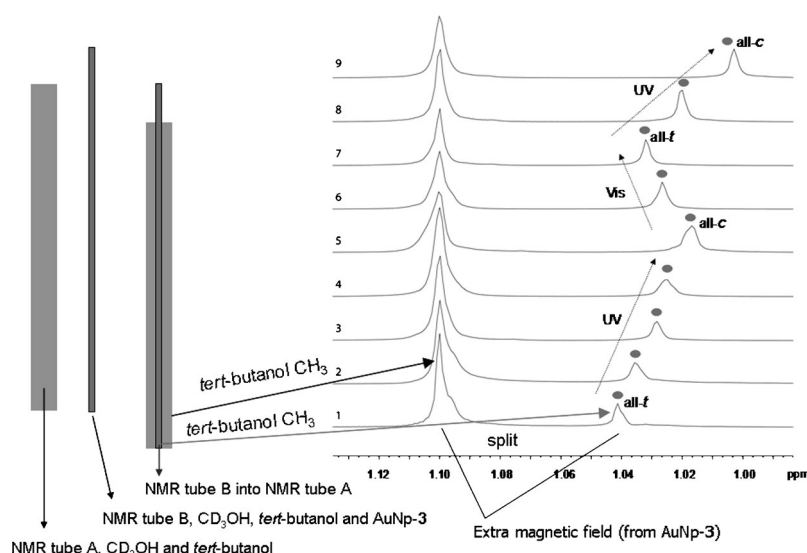


Figure 5. Modulation of the magnetic susceptibility of AuNp-3. Outer compartment (tube A): 4% *tert*-butanol in CD<sub>3</sub>OH. Inner compartment (tube B): 4% *tert*-butanol and 2.5 mg mL<sup>-1</sup> AuNp-3 in CD<sub>3</sub>OH (the resonance signals of CD<sub>3</sub>OH are not shown). Spectrum 1, all-*t* conformation for AuNp-3. From spectrum 2 to spectrum 5, four different periods of irradiation with UV light. Spectra 6 and 7 were recorded after two different times of irradiation with Vis light. Spectra 8 and 9 were recorded after two different times of irradiation with UV light.

portional to the relative difference (in Hz) between the two signals. It is clear from the graph that the behavior of  $\chi$  is strongly correlated to the isomerization of **3** (as a grafted ligand). In detail, starting from the all-*t* conformation for AuNp-3, upon irradiation at 350 nm the value of  $\chi$  increased to a maximum corresponding to the all-*c* conformation (this value did not change under prolonged photoillumination). Then, upon irradiation at 450 nm, the  $\chi$  value reversibly decreased, down to almost its initial value. This behavior was reproducible for several switches (2 cycles are shown in Figure 5) between the UV and Vis irradiation wavelengths.

In summary, two new C<sup>α</sup>-tetrasubstituted  $\alpha$ -amino acids, each characterized by the presence of two identical azobenzene-derived side chains, have been synthesized and found to exhibit photoreversible isomerization properties. A detailed analysis revealed the formation of intermediate chiral species during the isomerization process driven by light. These intermediate species were unambiguously detected as diastereomers when the bis(azobenzene)-containing amino acid was coupled to a chiral protein amino acid. Supramolecular systems formed by conjugation of one of the bis(azobenzene)-derived amino acids with different metal nanoparticles have been shown to retain the reversible photoswitch properties. Furthermore, the Au-derived nanoparticles exhibit a magnetic susceptibility dependence on the light-driven isomerization state that can be simply detected by <sup>1</sup>H NMR spectroscopy. Based on this behavior, these amino acids are of relevant potential for the development of a novel class of materials.

## Acknowledgements

Financial support from the Ministerio de Ciencia e Innovación (grant CTQ2010-17436, FPU fellowship to P. F.), the University of Padova ("Progetto Strategico" HELIOS 2008, prot. STPD08RCX), and the "Scientific Equipment for Research" Initiative (Oxford Gemini diffractometer) is gratefully acknowledged. M. C. thanks Prof. A. Dolmella for his help with X-ray diffraction data collection and processing.

**Keywords:** amino acids • azobenzene • magnetic properties • nanomaterials • prochirality

- [1] a) *Molecular Switches* (Ed: B. Feringa), Wiley-VCH, Weinheim, **2003**; b) E. R. Kay, D. A. Leigh, F. Zerbetto, *Angew. Chem.* **2007**, *119*, 72–196; *Angew. Chem. Int. Ed.* **2007**, *46*, 72–191; c) J. Andréasson, U. Pischel, *Chem. Soc. Rev.* **2010**, *39*, 174–188; d) A. P. de Silva, T. P. Vance, M. E. S. West, G. D. Wright, *Org. Biomol. Chem.* **2008**, *6*, 2468–2481; e) V. Balzani, A. Credi, M. Venturi, *Chem. Soc. Rev.* **2009**, *38*, 1542–1550; f) A. P. de Silva, H. Q. N. Gunaratne, T. Gunnlaugsson, A. J. M. Huxley, C. P. McCoy, J. T. Rademacher, T. E. Rice, *Chem. Rev.* **1997**, *97*, 1515–1566; g) V. Balzani, A. Credi, F. Raymo, J. F. Stoddart, *Angew. Chem.* **2000**, *112*, 3484–3530; *Angew. Chem. Int. Ed.* **2000**, *39*, 3348–3391.
- [2] a) Z. E. Liu, K. Hashimoto, A. Fujishima, *Nature* **1990**, *347*, 658–660; b) S. Zahan, J. W. Canary, *Angew. Chem.* **1998**, *110*, 321–323; *Angew. Chem. Int. Ed.* **1998**, *37*, 305–307; c) N. P. M. Huck, W. F. Jager, B. de Lange, B. Feringa, *Science* **1996**, *273*, 1686–1688; d) E. M. Nolan, S. J. Lippard, *Acc. Chem. Res.* **2009**, *42*, 193–203; e) Y. Takashima, V. Martínez, S. Furukawa, M. Kondo, S. Shimomura, H. Uehara, M. Nakahama, K. Sugimoto, S. Kitagawa, *Nat. Commun.* **2011**, *2*, 168; f) H. F. Yu, T. Ikeda, *Adv. Mater.* **2011**, *23*, 2149–2180; g) A. K. Cheetham, C. N. R. Rao, R. K. Feller, *Chem. Commun.* **2006**, 4780–4795; h) R. M. Cheetham, J. P. Bramble, D. G. G. McMillan, L. Krzeminski, X. Han, B. R. G. Johnson, R. J. Bushby, P. D. Olmsted, L. J. C. Jeuken, S. J. Marritt, J. N. Butt, S. D. Evans, *J. Am. Chem. Soc.* **2011**, *133*, 6521–6524.
- [3] a) M. Suda, N. Kameyama, M. Suzuki, N. Kawamura, Y. Einaga, *Angew. Chem.* **2008**, *120*, 166–169; *Angew. Chem. Int. Ed.* **2008**, *47*, 160–163; b) R. Klajn, J. F. Stoddart, B. A. Grzybowski, *Chem. Soc. Rev.* **2010**, *39*, 2203–2237; c) A. Ikegami, M. Suda, T. Watanabe, Y. Einaga, *Angew. Chem.* **2010**, *122*, 382–384; *Angew. Chem. Int. Ed.* **2010**, *49*, 372–374.
- [4] R. Klajn, *Pure Appl. Chem.* **2010**, *82*, 2247–2279.
- [5] a) T. E. Schrader, T. Cordes, W. J. Schreier, F. O. Koller, S.-L. Dong, L. Moroder, W. Zinth, *J. Phys. Chem. B* **2011**, *115*, 5219–5226; b) A. A. Beharry, L. Wong, V. Tropepe, G. A. Woolley, *Angew. Chem. Int. Ed.* **2011**, *50*, 1325–1327; c) E. H. G. Backus, R. Bloem, P. M. Donaldson, J. A. Ihalainen, R. Pfister, B. Paoli, A. Caffish, P. Hamm, *J. Phys. Chem. B* **2010**, *114*, 3735–3740; d) Z. Yu, S. Hecht, *Angew. Chem. Int. Ed.* **2011**, *50*, 1640–1643; e) M. Böckmann, N. L. Doltsinis, D. Marx, *Angew. Chem.* **2010**, *122*, 3454–3456; *Angew. Chem. Int. Ed.* **2010**, *49*, 3382–3384; f) F. Bonardi, G. London, N. Nouwen, B. L. Feringa, A. J. M. Driessen, *Angew. Chem.* **2010**, *122*, 7392–7396; *Angew. Chem. Int. Ed.* **2010**, *49*, 7234–7238; g) S.

- Martin, W. Haiss, S. J. Higgins, R. J. Nichols, *Nano Lett.* **2010**, *10*, 2019–2023; h) N. Hosono, T. Kajitani, T. Fukushima, K. Ito, S. Sasaki, M. Takata, T. Aida, *Science* **2010**, *330*, 808–811; i) S. Venkataramani, U. Jana, M. Dommaschk, F. D. Sönnichsen, F. Tuczek, R. Herges, *Science* **2011**, *331*, 445–448; j) P. K. Hashim, R. Thomas, N. Tamaoki, *Chem. Eur. J.* **2011**, *17*, 7304–7312.
- [6] a) M. Crisma, G. Valle, G. M. Bonora, C. Toniolo, F. Lelj, V. Barone, F. Fraternali, P. M. Hardy, H. L. S. Maia, *Biopolymers* **1991**, *31*, 637–641; b) E. Benedetti, B. Di Blasio, V. Pavone, C. Pedone, C. Toniolo, M. Crisma, *Biopolymers* **1992**, *32*, 453–456; c) M. Crisma, F. Formaggio, A. Moretto, C. Toniolo, *Biopolymers* **2006**, *84*, 3–12.
- [7] It is worth noting that the  $-C^{\beta}H_2-$  protons in the all-*c* and all-*t* isomers are an example of chemically non-equivalent protons occurring in a non-chiral molecule. See for example, M. H. Levitt, *Spin Dynamics. Basics of Nuclear Magnetic Resonance*, 1st ed., Wiley, Chichester, **2001**, p. 229.
- [8] I. M. Rio-Echevarria, R. Tavano, V. Causin, E. Papini, F. Mancin, A. Moretto, *J. Am. Chem. Soc.* **2011**, *133*, 8–11.
- [9] H. Ishii, K. Sugiyama, E. Ito, K. Seki, *Adv. Mater.* **1999**, *11*, 605–625.
- [10] a) D. F. Evans, *J. Chem. Soc.* **1959**, 2003–2005; b) J. Loliger, R. Scheffold, *J. Chem. Educ.* **1972**, *49*, 646–647.

Received: August 22, 2011  
Published online: September 28, 2011